Dyes and Pigments 82 (2009) 244–250

Contents lists available at ScienceDirect

Dyes and Pigments

journal homepage: www.elsevier.com/locate/dyepig

The synthesis and photophysicochemical behaviour of novel water-soluble cationic indium(III) phthalocyanine

Mahmut Durmuş [a], Ali Erdoğmuş [b,c], Abimbola Ogunsipe [b,d], Tebello Nyokong [b,*]

[a] Gebze Institute of Technology, Department of Chemistry, P.O. Box 141, Gebze 41400, Turkey
[b] Department of Chemistry, Rhodes University, Grahamstown 6140, South Africa
[c] Yıldız Technical University, Faculty of Arts and Science, Department of Chemistry, 34210 Esenler, Istanbul, Turkey
[d] Department of Chemistry, University of Lagos, Lagos, Nigeria

ARTICLE INFO

Article history:
Received 9 November 2008
Received in revised form
12 January 2009
Accepted 16 January 2009
Available online 27 January 2009

Keywords:
Indium(III) phthalocyanine
Synthesis
Photophysics
Photochemistry
Photodynamic therapy
Singlet oxygen

ABSTRACT

The syntheses and characterization of 2,3-octakis-(3-pyridyloxyphthalocyaninato) indium(III) and quaternized 2,3-octakis-(3-pyridyloxyphthalocyaninato) indium(III) are described. The ground state electronic absorption spectra, photophysics and photochemistry of both dyes in DMSO as well as that of the quaternized compound in aqueous solution are also presented. A comparison of the photophysical and photochemical parameters of the two dyes revealed that quaternized 2,3-octakis-(3-pyridyloxyphthalocyaninato) indium(III) was a better photosensitizer than its unquaternized counterpart. The quantum yield values of fluorescence (Φ_F), triplet state formation (Φ_T) and singlet oxygen formation (Φ_Δ) for the cationic dye were found to be 0.03, 0.68 and 0.66 respectively in DMSO; these values were higher than those for 2,3-octakis-(3-pyridyloxyphthalocyaninato) indium(III), which exhibited values of 0.02, 0.66 and 0.63, respectively in DMSO. The values for the cationic dye in aq. solution were 0.02, 0.59 and 0.56 respectively, suggesting that the water-soluble quaternized 2,3-octakis-(3-pyridyloxyphthalocyaninato) indium(III) offers potential as a photosensitizer in photodynamic therapy treatment.

1. Introduction

Phthalocyanines (Pcs) are an interesting class of compounds which exhibit both chemical and physical stabilities [1–3]. The Pc macrocycle can engage most metal ions in its cavity; hence scores of different metallophthalocyanines (MPcs) have been synthesized. The nature of the metal ion encapsulated within the Pc cavity plays a vital role in the properties, reactions and of course, applications of the resulting MPc. MPcs exhibit a wide range of applications ranging from industrial [4,5], technological [6–8] to medical [9,10]. MPc derivatives in which the central metal is diamagnetic and non-transitional are photoactive, and are often employed in photosensitization and energy conversion [11–13]. Worth emphasizing is the Pcs' application as photosensitizers (PSs) in the photodynamic therapy (PDT) of tumours. The photophysics and photochemistry of InPc derivatives are well documented [14–17]. Such studies reveal that these complexes show great promise for photocatalytic and photosensitizing applications [18,19]. However, studies on water-soluble indium phthalocyanine (InPc) derivatives are scarce in the literature [20]. In PDT administration, the drug is injected into the patient's blood stream, and since the blood itself is a hydrophilic system, water solubility becomes crucial for a potential PS in PDT.

The advantages of MPcs bearing cationic substituents over those with neutral and anionic substituents are numerous [21], and include the following: (i) they are able to improve water solubility and prevent aggregation [22,23]; aggregation seriously compromises the PDT value of the PS, (ii) they are more efficient as PDT agents [24–26] and also improve cell uptake [27], (iii) they are selectively localized in the cell mitochondria, which when impaired induces apoptosis [28,29]. The advantages that go with cation-substituted MPcs are too striking to overlook, hence our interest in these complexes. In this work, the synthesis, photophysical and photochemical studies on new water-soluble cationic octasubstituted indium phthalocyanine derivative (Scheme 1) are presented.

During PDT, singlet oxygen is the predominant cytotoxic agent produced. Singlet oxygen is produced when the PS undergoes electronic excitation from a ground singlet (S_0) state to an excited singlet (S_1) state; the S_1 state is highly unstable, and rapidly undergoes intersystem crossing to a longer-lived excited triplet (T_1) state. One of the few chemical species present in tissue is triplet state oxygen. When the PS and an oxygen molecule are in

* Corresponding author. Tel.: +27 46 6038260; fax: +27 46 6225109.
E-mail address: t.nyokong@ru.ac.za (T. Nyokong).

0143-7208/$ – see front matter © 2009 Elsevier Ltd. All rights reserved.
doi:10.1016/j.dyepig.2009.01.008

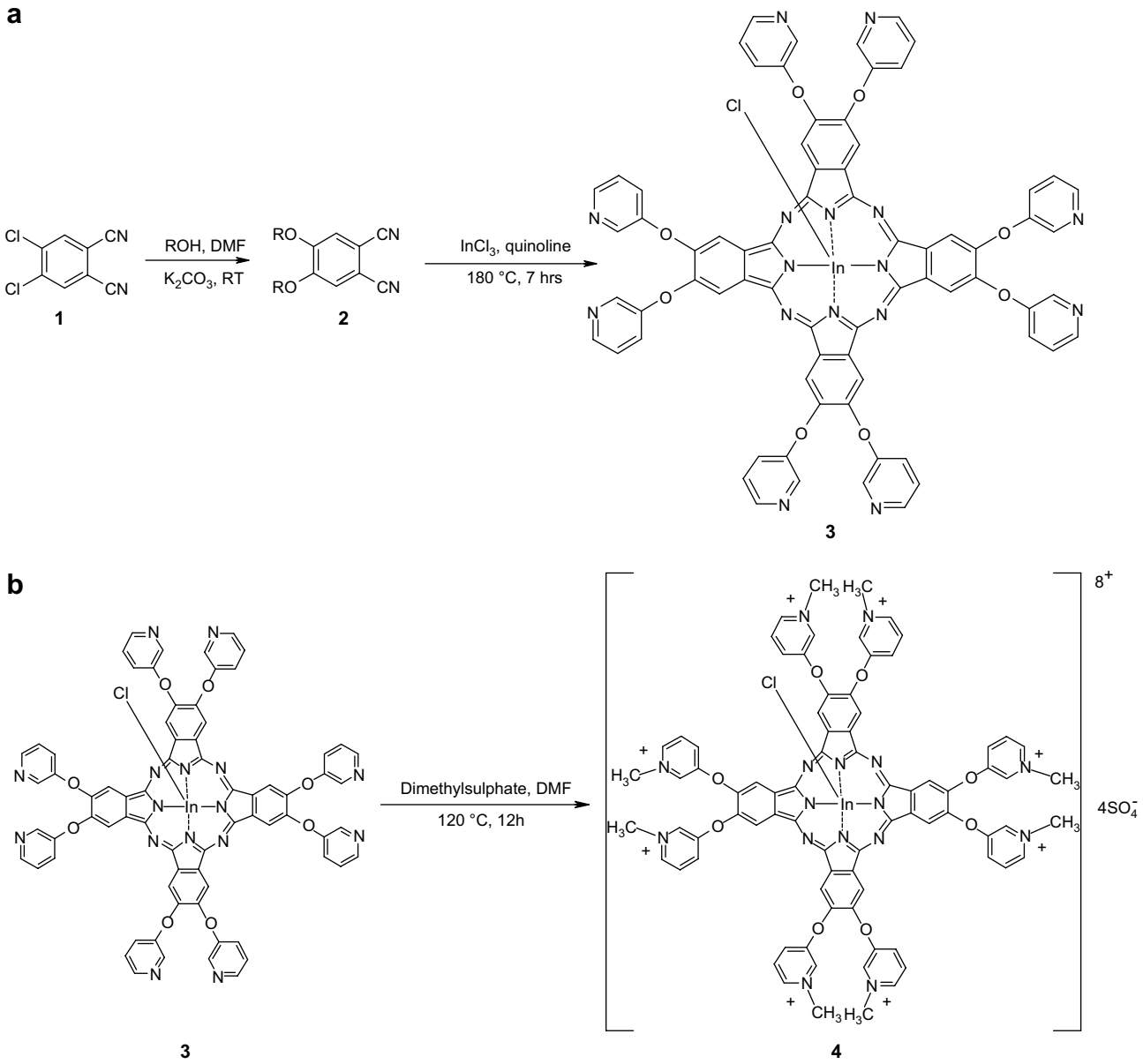

Scheme 1. a: Synthesis of octa-3-pyridyloxy substituted (phthalocyaninato) indium(III). b: Synthesis of quaternized octa-3-pyridyloxy substituted (phthalocyaninato) indium(III).

proximity, energy transfer can take place. It is this energy that is responsible for the spin inversion in molecular oxygen. In the light of this, a high yield of the PS's triplet state (and a concomitant high yield of singlet oxygen) is crucial for the choice of a PS in PDT. In order to assess its compatibility with this technique, a thorough photophysicochemical study on a potential PS is highly desirable. Thus this work investigates important photophysical and photochemical properties of the InPc derivatives, as shown in Scheme 1.

2. Experimental

2.1. Materials

Zinc(II) phthalocyanine (ZnPc), chlorophyll *a*, 1,3-diphenylisobenzofuran (DPBF) were purchased from Aldrich and zinc tetrasulfophthalocyanine ($ZnPcS_4$) was synthesized according to literature method [30]. Quinoline, dimethylsulphoxide (DMSO, SAARCHEM) and dimethylformamide (DMF, SAARCHEM) were dried as described by Perrin and Armarego [31] before use. Methanol, *n*-hexane, chloroform ($CHCl_3$), dichloromethane (DCM), tetrahydrofuran (THF), acetone, ethanol were freshly distilled. Indium(III) chloride, K_2CO_3, 3-hydroxypyridine, dimethylsulphate (DMS) and Triton X-100 were purchased from Aldrich. 9,10-Antracenediyl-bis(methylene)dimalonic acid (ADMA) was purchased from Fluka. Preparative thin layer chromatography was performed on silica gel 60 P F_{254}. 4,5-Dichlorophthalonitrile (**1**) [32] and 4,5-bis(3-pyridyloxy)phthalonitrile (**2**) [33] were synthesized and purified according to literature procedures.

2.2. Equipment

UV–vis spectra were recorded on a Cary 500 UV–vis/NIR spectrophotometer. Fluorescence excitation and emission spectra were recorded on a Varian Eclipse spectrofluoremeter using 1 cm path length cuvettes at room temperature. Elemental analyses were obtained with a Thermo Finnigan Flash 1112 Instrument. IR spectra (KBr pellets) were recorded on a Bio-Rad FTS 175C FTIR spectrometer. ^1H NMR spectra were recorded in DMSO-d_6 solutions on

a Varian 500 MHz spectrometer. Positive ion and linear mode MALDI-MS of complexes were obtained in 1,8,9-anthracenetriol for non-ionic complex (**3**) and dihydroxybenzoic acid for ionic complex (**4**) as MALDI matrix using nitrogen laser accumulating 50 laser shots using Bruker Microflex LT MALDI-TOF mass spectrometer.

Triplet absorption and decay kinetics were recorded on a laser flash photolysis system; the excitation pulses were produced by a Nd:YAG laser (Quanta-Ray, 1.5 J/8 ns) pumping a dye laser (Lambda Physic FL 3002, Pyridin 1 in methanol). The analyzing beam source was from a Thermo Oriel xenon arc lamp, and a photomultiplier tube was used as detector. Signals were recorded with a two-channel digital real-time oscilloscope (Tektronix TDS 360); the kinetic curves were averaged over 256 laser pulses. Triplet lifetimes were determined by exponential fitting of the kinetic curves using OriginPro 7.5 software. Fluorescence lifetimes were determined using the program PhotochemCAD [34], and the determination is based on the Strickler–Berg equation [35].

2.3. Synthesis

2.3.1. 2,3-Octakis-(3-pyridyloxyphthalocyaninato) indium(III) (**3**, Scheme 1a)

A mixture of anhydrous indium(III) chloride (1.06 g, 4.77 mmol), 4,5-bis(3-pyridyloxy)phthalonitrile (**2**) (3.00 g, 9.55 mmol) and quinoline (5 ml, doubly distilled over CaH_2) was stirred at 180 °C for 7 h under nitrogen atmosphere. After cooling, the solution was dropped in *n*-hexane. The green solid product was precipitated and collected by filtration and washed with *n*-hexane. The crude product was dissolved in DMF. After concentrating, the dark green waxy product was precipitated with hot ethanol and washed with ethanol, acetone, $CHCl_3$, *n*-hexane and diethylether. Furthermore this product was purified with preparative thin layer chromatography (silica gel) using THF–MeOH (1:1) solvent system. Yield: 1.95 g (58%). UV–vis (DMSO): λ_{max} nm (log ε) 359 (4.66), 619 (4.32), 691 (5.05). IR [(KBr) ν_{max}/cm^{-1}]: 3073 (Ar–CH), 1572 (C=C), 1477, 1433, 1393, 1259, 1099 (C–O–C), 995, 741, 705. ^{1}H NMR (DMSO-d_6): δ, ppm 9.30 (8H, br, Pyridyl-H), 9.16 (8H, s, Pyridyl-H), 8.93 (8H, s, Pc-H), 8.23 (8H, d, Pyridyl-H), 7.95 (8H, d, Pyridyl-H). Calc. for $C_{72}H_{40}ClN_{16}O_8In$: C 61.44, H 2.86, N 15.92; Found: C 60.92, H 2.74, N 16.49. MALDI-TOF-MS *m*/*z*: Calc. 1407.48; Found (M + Na) 1431.09.

2.3.2. Quaternized 2,3-octakis-(3-pyridyloxyphthalocyaninato) indium (III) (**4**, Scheme 1b)

This complex was prepared according to the method previously reported by Smith et al. [36]. Compound **3** (500 mg, 0.35 mmol) was heated to 120 °C in freshly distilled DMF (5 ml) and excess dimethylsulphate (0.1 ml) was added dropwise. The mixture was stirred at 120 °C for 12 h. After this time, the mixture was cooled to room temperature and the product was precipitated with hot acetone and collected by filtration. The green solid product was washed successively with hot ethanol, ethyl acetate, THF, chloroform, *n*-hexane and diethylether. The resulting hygroscopic product was dried over phosphorous pentoxide. Yield: 0.55 g (82%). UV–vis (DMSO): λ_{max} nm (log ε) 358 (4.35), 616 (4.01), 686 (4.71). IR [(KBr) ν_{max}/cm^{-1}]: 3057 (Ar–CH), 2960 (CH), 1589 (C=C), 1505, 1399, 1279 (S=O), 1194 (S=O), 743, 600 (S–O). ^{1}H NMR (D_2O): δ, ppm 9.21–7.58 (40H, m, Pc-H and Pyridyl-H), 4.24 (24H, s, CH_3). Calc. for $C_{80}H_{72}ClN_{16}O_{28}S_4In$ (+4H_2O): C 48.43, H 3.66, N 11.30; Found: C 48.11, H 3.24, N 11.98. MALDI-TOF-MS *m*/*z*: Calc. 1910; Found (M − InCl) 1760.02.

2.4. Fluorescence quantum yields and lifetimes

Fluorescence quantum yields (Φ_F) were determined by the comparative method [37,38] (Equation (1)), using chlorophyll *a* in ether ($\Phi_F = 0.32$) [39] as the reference.

$$\Phi_F = \Phi_F(\mathrm{Std})\frac{F_x \cdot A_{Std} \cdot n_x^2}{F_{Std} \cdot A_x \cdot n_{Std}^2} \quad (1)$$

where F_x and F_{Std} are the areas under the fluorescence emission curves of the sample and standard, respectively. A_x and A_{Std}, the absorbances of the sample and standard, respectively; and n_x and n_{Std}, the refractive indices of the solvents used for sample and standard, respectively. Both the sample and the reference were excited at the same wavelength. The absorbance of the solutions at the excitation wavelength ranged between 0.04 and 0.05.

2.5. Triplet quantum yields and lifetimes

The solutions for triplet state quantum yields and lifetimes were introduced into a 1 cm path length UV–vis spectrophotometric cell, deaerated using nitrogen and irradiated at the Q band maxima. Triplet state quantum yields (Φ_T) were determined by triplet–triplet absorption method. A comparative method [40] using ZnPc (in DMSO; $\Phi_T^{Std} = 0.65$ [41]) and $ZnPcS_4$ (in H_2O; $\Phi_T^{Std} = 0.56$ [42]) as standards, was employed for the calculations, Eq. (2).

$$\Phi_T = \Phi_T^{Std} \cdot \frac{\Delta A_T \cdot \varepsilon_T^{Std}}{\Delta A_T^{Std} \cdot \varepsilon_T} \quad (2)$$

where ΔA_T and ΔA_T^{Std} are the changes in the triplet state absorbances of the InPc derivative and the standard respectively; ε_T and ε_T^{Std}, the triplet state molar extinction coefficients for the InPc derivative and the standard respectively; ε_T and ε_T^{Std} were determined from the molar extinction coefficients of their respective ground singlet states (ε_S and ε_S^{Std}) and the changes in absorbances of the ground singlet states (ΔA_S and ΔA_S^{Std}), according to Equation (3) [43]:

$$\varepsilon_T = \varepsilon_S \cdot \frac{\Delta A_T}{\Delta A_S} \quad (3)$$

quantum yields of internal conversion (Φ_{IC}) were obtained from Equation (4), which assumes that only the three intrinsic processes (fluorescence, intersystem crossing and internal conversion), jointly deactivate the excited singlet state of an InPc molecule.

$$\Phi_{IC} = 1 - (\Phi_F + \Phi_T) \quad (4)$$

2.6. Singlet oxygen and photodegradation quantum yields

Singlet oxygen and photodegradation quantum yields of the InPc complexes were determined as previously explained in detail [44–46]. Typically, a 2 ml reaction solution was introduced into the cell and irradiated in the Q band region of the respective InPc derivative with a General Electric Quartz line lamp (300 W). A 600 nm glass cut off filter (Schott) and a water filter were used to filter off ultraviolet and infrared radiations. An interference filter (Intor, 690 nm with a band width of 40 nm) was additionally placed in the light path before the sample. Singlet oxygen quantum yields (Φ_Δ) were determined in air using the relative method with ZnPc (in DMSO) and ZnTSPc (in water) as references; and DPBF and ADMA respectively as chemical quenchers for singlet oxygen, using Equation (5):

$$\Phi_\Delta = \Phi_\Delta^{Std} \cdot \frac{R_{DPBF} \cdot I_{abs}^{Std}}{R_{DPBF}^{Std} \cdot I_{abs}} \quad (5)$$

where Φ_Δ^{Std} is the singlet oxygen quantum yield for the standard {ZnTSPc ($\Phi_\Delta^{Std} = 0.56$ in aqueous solution [47]) and ZnPc ($\Phi_\Delta^{Std} = 0.67$ in DMSO [48])}; *R* and R^{Std} are the ADMA or DPBF

photobleaching rates in the presence of the respective InPc derivative and standard, respectively; I_{abs} and I_{Abs}^{Std} are the rates of light absorption by the InPc derivative and standard, respectively. The concentrations of ADMA and DPBF in the solutions were calculated using the determined values of $\log \varepsilon = 4.10$ at 380 nm (ADMA in aqueous solution) and $\log \varepsilon = 4.36$ at 417 nm (DPBF in DMSO). The light intensity used for Φ_Δ determinations was found to be 5.35×10^{15} photons s^{-1} cm^{-2} for both standards and samples. The absorbance values of both standards and samples were also kept the same.

For determination of photobleaching quantum yields, the usual Equation (6) [49,50] was employed:

$$\Phi_{Pd} = \frac{(C_0 - C_t)\cdot V \cdot N_A}{I_{abs}\cdot S \cdot t} \quad (6)$$

where C_o and C_t (mol dm^{-3}) are the InPc derivatives' concentrations before and after irradiation respectively; V, the reaction volume; S, the irradiated cell area (2.0 cm^2); t, the irradiation time; N_A, Avogadro's number and I_{abs}, the overlap integral of the radiation source intensity and the absorption of the Pc (the action spectrum) in the region of the interference filter transmittance.

At least three independent experiments were performed for the quantum yield determinations, and the error in the determination was ~10%.

3. Results and discussion

3.1. Syntheses and characterization

The preparation of phthalocyanine derivatives from the aromatic nitriles occurs under different reaction conditions. The synthesis of indium phthalocyanine complex (**3**) was achieved by treatment of phthalonitrile **2** with anhydrous $InCl_3$ in freshly distilled quinoline (Scheme 1a). Because indium is a large atom, high energy is required to insert the metal ion into the phthalocyanine cavity ring, thus a high-boiling solvent (such as quinoline or 1-chloronaphthalene) is used to achieve this purpose. Preparative thin layer chromatography with silica gel was employed to obtain the pure products from the reaction mixtures.

Quaternizations of the indium phthalocyanine compound was achieved by reaction with excess dimethylsulphate (DMS) as quaternization agent in DMF at 120 °C. Yield of the product was 82% for **4**. After reaction with DMS, the quaternized complex is very soluble in water.

Generally, phthalocyanine complexes are insoluble in most organic solvents and water; however introduction of substituents on the ring increases the solubility. Complexes **3** and **4** exhibited excellent solubility in DMF and DMSO. Quaternized complex (**4**) is soluble in water as well. The new compounds were characterized by UV–vis, IR and ^{1}H NMR spectroscopies, MALDI-TOF mass spectra and elemental analysis. The analyses are consistent with the predicted structures as shown in the Experimental section. The characteristic vibrations corresponding to ether groups (C–O–C) at *ca.* 1099 cm^{-1}, aromatic CH stretching at 3073–3057 cm^{-1} were observed for all complexes. Aliphatic CH stretching at *ca.* 2960 cm^{-1}, S=O stretching at 1279 cm^{-1} and 1194 cm^{-1}, S–O stretching at 600 cm^{-1} for **4** are indicative of quaternization formation.

The complexes were found to be pure by ^{1}H NMR with all the substituents and ring protons observed in their respective regions. The resonance belonging to ring protons was observed as a singlet peak at 8.93 ppm for **3** integrating for 8 protons. The pyridyloxy protons were observed as broad peaks at 9.30 ppm, as a singlet at 9.16 ppm and as doublets at 8.23 ppm and 7.95 ppm integrating for 8, 8, 8, 8 protons each, respectively, making a total of 32 protons as expected. Although the presence of phthalocyanine aggregation at the concentrations used for the NMR measurements may lead to broadening of the aromatic signals [51], the observed spectra of the complexes were relatively well resolved.

The NMR spectra of the quaternized phthalocyanine complex (**4**) showed less resolved patterns compared to non-quaternized derivatives. This complex (**4**) showed the phthalocyanine ring protons and pyridyl group protons as unresolved multiplets between 9.21 and 7.58 ppm integrating for a total of 40 protons. The methyl protons which integrated for 24 protons were observed at 4.24 ppm for quaternized complex (**4**) as a singlet.

3.2. UV–vis absorption and fluorescence spectra

Fig. 1 shows the UV–vis absorption spectra of **3** and **4** in DMSO; the well defined Q band maxima at 691 nm (**3**) and 686 nm (**4**) (Table 1) are usual for monomeric phthalocyanine complexes [1]. The Soret bands of these complexes exist at ~357 nm (Fig. 1 inset), and are broad due to incomplete merging of the B_1 and B_2 bands. The Q and B (Soret) bands both arise from π–π^* transitions and can be explained in terms of linear combination of transitions from a_{1u} (Q) and a_{2u}/b_{2u} (B) HOMO orbitals to the doubly degenerate e_g (LUMO) orbitals. The slight broadening of the Q bands of **3** and **4** may be attributed to steric effects of the substituents at the peripheral positions, which results in a slight deviation of the Pc skeleton from planarity [52]. Such departure from planarity is common in tetraphenyl porphyrins [52]. It is also known that the presence of eight phenyl groups on the peripheral positions of the phthalocyanine ring results in high distortion of the ring [53]. The Q band position of **3** in DMSO is red-shifted by 5 nm relative to that of **4**. The lone pair of the tertiary nitrogen atom of the substituent in **3** is delocalized into the ring, thereby raising the HOMO energy, and ultimately leading to a red-shifting. However when this lone pair is engaged as in **4**, its mesomeric contribution to the ring electron density is lost, which results in a slight lowering of the HOMO and an attendant blue-shifting in the Q band position. In water, the absorption spectrum of **4** shows cofacial aggregation, as evidenced by the presence of two non-vibrational peaks in the Q band region, Fig. 2(i), Table 1. The lower energy (red-shifted) band at 673 nm is due to the monomeric species, while the higher energy (blue-shifted) band at 640 nm is due to the aggregated species. Addition of a drop of Triton X-100 to an aqueous solution of **4** brought about considerable increase in intensity of the low energy side of

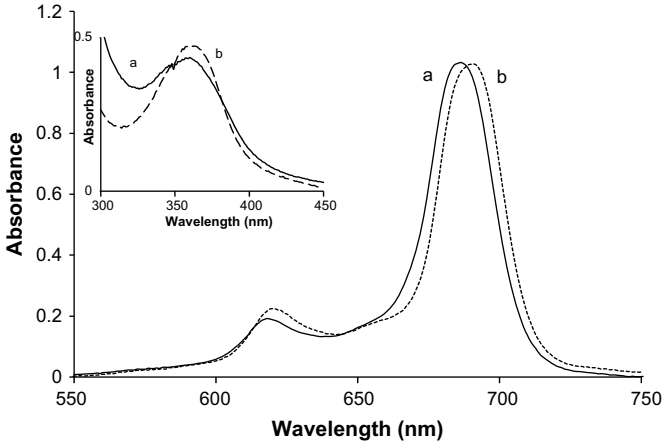

Fig. 1. UV–vis absorption spectra of (a) **3** (1.93×10^{-5} M) and (b) **4** (8.95×10^{-6} M) in DMSO.

Table 1
Spectral parameters of **3** and **4** in DMSO and water.[a]

	Solvent	$\lambda_{Q\text{-}Abs}$/nm (log ε)	$\lambda_{Q\text{-}Exc}$/nm	$\lambda_{Q\text{-}Em}$/nm	$\Delta\lambda$ (Stokes)/nm
3	DMSO	691 (5.05)	686	702	16
4	DMSO	686 (4.71)	685	703	18
4	Water	640 (4.47), 673 (4.32)	687	700	13
4	Water + Triton X-100	685 (4.65)	687	700	13

[a] $\lambda_{Q\text{-}Abs}$, $\lambda_{Q\text{-}Exc}$ and $\lambda_{Q\text{-}Em}$ are the wavelengths of maximum absorption, excitation and emission, respectively; and $\Delta\lambda$, Stokes' shift.

the Q band (Fig. 2(ii)), suggesting that addition of Triton X-100 breaks up the aggregates. However, some aggregated portions of **4** still remained in solution even after addition of Triton X-100, as shown in Fig. 2. Aggregated MPcs exhibit limited applicability in photocatalysis because the aggregates convert electronic excitation energy into vibrational energy, due to the closeness of the individual molecules; thereby reducing the excited state lifetimes of the complexes. In this work, photophysical and photochemical studies on **4** in aqueous solution were carried out in the presence of Triton X-100 to hinder aggregation, as seen in Fig. 2(ii). The Q band position of **4** in water (685 nm, in the presence of Triton X-100) is almost the same as that in DMSO (Table 1), suggesting that solvent effect on the spectral position of this complex is insignificant. Fig. 3 shows the absorption (b), fluorescence excitation (a) and fluorescence emission (c) spectra of **4** in DMSO. The fluorescence excitation spectrum is slightly blue-shifted by 1 nm relative to the absorption spectrum, this is an insignificant shift, and could have been caused by different spectrometers (one used for fluorescence versus the one used for absorption) and/or different settings of the spectrometer slit widths. The absorption and fluorescence excitation spectra of **3** in DMSO are similar (figure not shown). Stokes' shifts were calculated from the absorption bands that populate the fluorescent state, i.e. excitation wavelength. Stokes' shift ranged from 13 to 18 nm, thus they were very close to one another.

3.3. Photophysical parameters

3.3.1. Fluorescence quantum yields and lifetimes

The fluorescence quantum yields (Φ_F) of **3** (in DMSO) and **4** (in DMSO and water) are given in Table 2. The value for **3** ($\Phi_F = 0.02$) is not too different from that for **4** considering experimental error (± 0.01). Excited singlet state lifetime refers to the average time a molecule stays in its excited state. Any factor that shortens the excited singlet state lifetime of a fluorophore indirectly reduces the value of Φ_F. Such factors include internal conversion and intersystem crossing. As a result, the nature and the environment of a fluorophore determine its excited singlet state lifetime. In DMSO,

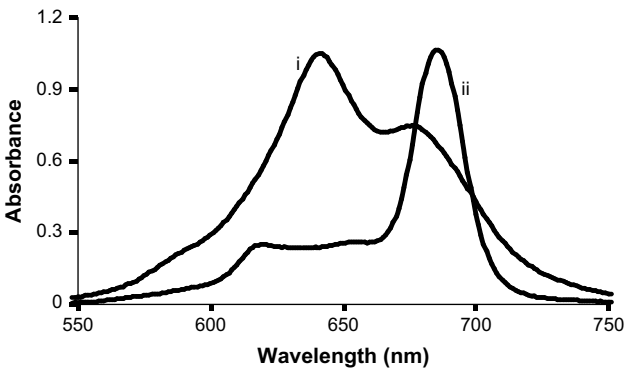

Fig. 2. UV–vis absorption spectra of **4** in water (i) and in water containing Triton X-100 (ii).

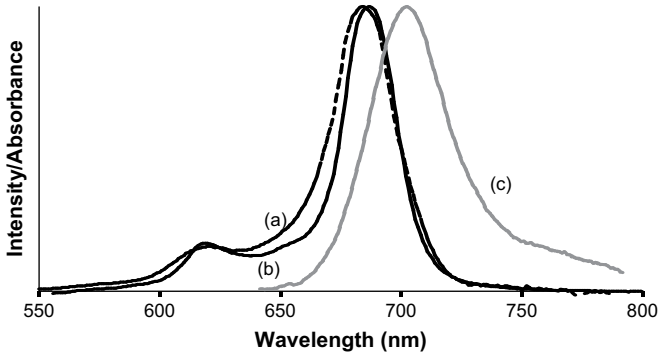

Fig. 3. Fluorescence excitation (a), UV–vis absorption (b) and fluorescence emission (c) spectra of **4** in DMSO.

the τ_F value of **4** ($\tau_F = 0.75$) is longer than that in water ($\tau_F = 0.44$) and that of **3** ($\tau_F = 0.41$) in DMSO.

3.3.2. Triplet quantum yields and lifetimes

Fig. 4 shows the transient difference absorption spectrum of **3** in DMSO. Each spectrum was recorded 10 μs after the flash. Φ_T value for **4** ($\Phi_T = 0.68$) is almost the same as that for **3** ($\Phi_T = 0.66$) in DMSO within experimental error, implying that quaternization slightly enhances intersystem crossing, as observed before [18]. In DMSO, Φ_T value for **4** (0.68) is larger than that in water ($\Phi_T = 0.59$), which is attributed to increased intermolecular interaction in water compared to that in DMSO. Even in the presence of Triton X-100, some level of aggregation still exists in water, as shown above, Fig. 2.

The triplet lifetimes of the complexes are listed in Table 2. The τ_T value is longer for **4** (150 μs) than for **3** (80 μs) in DMSO. The triplet lifetime of **4** is longer in DMSO (150 μs) than in water (10 μs), and this is as well explained by remaining aggregation in water.

3.3.3. Singlet oxygen and photodegradation quantum yields

Singlet oxygen quantum yield (Φ_Δ) is a measure of the efficiency of singlet oxygen production. During singlet oxygen generation, the triplet state of a PS is intercepted by ground state molecular oxygen in the vicinity of the PS. It is therefore logical to interpret the trends in the variation of Φ_Δ values in terms of the population and lifetime of the PS's triplet state. The Φ_Δ values for **3** ($\Phi_\Delta = 0.63$) and **4** ($\Phi_\Delta = 0.66$) in DMSO are almost identical within experimental error (10%). This observation is not unexpected on grounds of closeness in the respective values of Φ_T. The slight disparity between these values could be attributed to differences in triplet lifetimes of the complexes. Comparing the Φ_Δ values for **4** in DMSO (0.66) and water (0.56), the smaller value in water is ascribed to the quenching of singlet oxygen by water, as demonstrated in the shorter lifetime of singlet oxygen in water (4.2 μs) [54] compared to that in DMSO (30 μs) [55].

Photodegradation quantum yield is a measure of the efficiency of degradation of an absorbing species as a result of photon absorption. Photodegradation is known to be a singlet oxygen-mediated process; hence it is not surprising that the variation of Φ_{Pd} in Table 2 follows the same trend as that of Φ_Δ, with Φ_{Pd} value being greater for **4** than for **3** in DMSO, and higher in DMSO than in water.

Table 2
Photophysical and photochemical parameters of **3** and **4** in DMSO and water.

	Φ_F	Φ_T	Φ_{IC}	Φ_Δ	$\Phi_{Pd}/10^{-5}$	τ_F/ns	τ_T/μs
3 (DMSO)	0.02	0.66	0.35	0.63	3.41	0.41	80
4 (DMSO)	0.03	0.68	0.31	0.66	40.0	0.75	150
4 (water + Triton X-100)	0.02	0.59	0.40	0.56	1.20	0.44	10

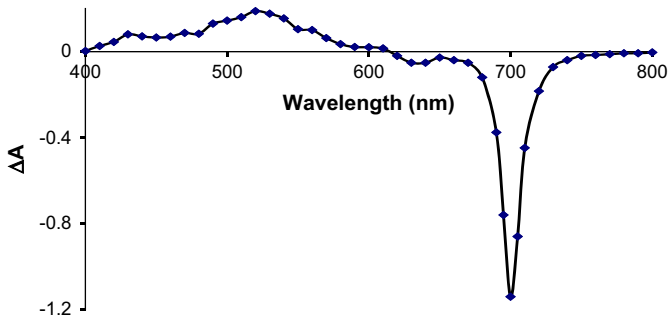

Fig. 4. Transient difference absorption spectrum of **3** in DMSO. Concentration = 2.89×10^{-5} M; Excitation wavelength = 691 nm.

4. Conclusions

In conclusion, this work has described the synthesis, spectral, photophysical and photochemical properties of two new substituted indium(III) phthalocyanine complexes. The effect of quaternization on these properties is also presented. We have shown that quaternization imparts water solubility and also enhances the photophysical and photochemical parameters of the InPc derivative. Solvent effect on the photophysical and photochemical properties of the quaternized derivative is investigated. Although, the photophysical and photochemical properties relevant for photosensitization gave more attractive values in DMSO, the values in water are still good enough for PDT applications. This work will certainly enrich the hitherto scanty literature on the potentials of cationic phthalocyanines as photosensitizers in PDT.

Acknowledgements

This work was supported by the Department of Science and Technology (DST) and National Research Foundation (NRF) of South Africa through DST/NRF South African Research Chairs Initiative for Professor of Medicinal Chemistry and Nanotechnology and Rhodes University.

References

[1] Leznoff CC, Lever ABP, editors. The phthalocyanines: properties and application, vols. I–IV. John Wiley and Sons, Inc.; 1986–1993.
[2] Mckeown NB. Phthalocyanine materials – synthesis, structure and function. Cambridge: Cambridge University Press; 1998.
[3] Kadish K, Smith KM, Guilard R, editors. The porphyrin handbook, vols. 15–20. Boston: Academic Press; 2003.
[4] Gregory P. Industrial applications of phthalocyanines. J Porphyrins Phthalocyanines 2000;4:432–7.
[5] Hohnholz D, Steinbrecher S, Hanack M. Applications of phthalocyanines in organic light emitting devices. J Mol Struct 2000;521:231–7.
[6] Daimon K, Nukada K, Sakaguchi Y, Igarashi R. A new polymorph of hydroxygallium phthalocyanine and its application in a photoreceptor. J Imaging Sci Technol 1996;40:249–53.
[7] El-Nahass MM, Farag AM, Abd El-Rahman KF, Darwish AAA. Dispersion studies and electronic transitions in nickel phthalocyanine thin films. Opt Laser Technol 2005;37:513–23.
[8] Tracz A, Makowski T, Masirek S, Pisula W, Geerts YH. Macroscopically aligned films of discotic phthalocyanine by zone casting. Nanotechnology 2007;18:485303–7.
[9] Priola SA, Raines A, Caughey WS. Porphyrin and phthalocyanine antiscrapie compounds. Science 2000;287:1503–6.
[10] Ben-Hur E, Chan WS, editors. Porphyrin handbook, vol. XIX. Boston: Academic Press; 2003. p. 1–35.
[11] Ben-Hur E, Green M, Prager A, Kol R, Rosenthal I. Phthalocyanine photosensitization of mammalian cells: biochemical and ultrastructural effects. Photochem Photobiol 1987;46:651–6.
[12] MacDonald IJ, Dougherty TJ. Basic principles of photodynamic therapy. J Porphyrins Phthalocyanines 2001;5:105–29.
[13] Lo P-C, Leng X, Ng DKP. Hetero-arrays of porphyrins and phthalocyanines. Coord Chem Rev 2007;251:2334–53.
[14] Wang S, Gan Q, Zhang Y, Li S, Xu H, Yang G. Optical-limiting and photophysical properties of two soluble chloroindium phthalocyanines with α- and β-alkoxyl substituents. ChemPhysChem 2006;7:935–41.
[15] Chen Y, Araki Y, Dini D, Liu Y, Ito O, Fujitsuka M. The steady-state and time-resolved photophysical properties of a dimeric indium phthalocyanine complex. Mater Chem Phys 2006;98:212–6.
[16] Chen Y, Dini D, Hanack M, Fujitsua M, Ito O. Excited state properties of monomeric and dimeric axially bridged indium phthalocyanines upon UV–vis laser irradiation. Chem Commun 2004:340–1.
[17] Chen Y, Araki Y, Fujitsuka M, Hanack M, Ito O, O'Flaherty SM, et al. Photophysical studies on axially substituted indium and gallium phthalocyanines upon UV–vis laser irradiation. Solid State Commun 2004;131:773–8.
[18] Ogunsipe A, Durmuş M, Nyokong T. Photophysical, photochemical and bovine serum albumin binding studies on water-soluble gallium(III) phthalocyanine derivatives. J Porphyrins Phthalocyanines 2007;11:635–44.
[19] Nagamura T, Adachi T, Yoshida I, Inoue H, Heckmann H, Hanack M. Ultrafast reflection control based on photoinduced complex refractive index changes in guided mode thin films containing indium phthalocyanine. Mol Cryst Liq Cryst 2001;370:97–102.
[20] Durmuş M, Nyokong T. Synthesis, photophysical and photochemical studies of new water-soluble indium(III) phthalocyanines. Photochem Photobiol Sci 2007;6:659–68.
[21] Zimcik P, Miletin M, Musil Z, Kopecky K, Kubza L, Brault D. Cationic azaphthalocyanines bearing aliphatic tertiary amino substituents – synthesis, singlet oxygen production and spectroscopic studies. J Photochem Photobiol A Chem 2006;183:59–69.
[22] Kudrevich SV, Galpern MG, van Lier JE. Synthesis of octacarboxytetra (2,3-pyrazino)porphyrazine: novel water soluble photosensitizers for photodynamic therapy. Synthesis 1994;8:779–81.
[23] de Filippis MP, Dei D, Fantetti L, Roncucci G. Synthesis of a new water-soluble octa-cationic phthalocyanine derivative for PDT. Tetrahedron Lett 2000;41:9143–7.
[24] Cruse-Sawyer JE, Griffiths J, Dixon B, Brown SB. The photodynamic response of two rodent tumour models to four zinc(II) substituted phthalocyanines. Br J Cancer 1998;77:965–72.
[25] Scalise I, Durantini EN. Synthesis, properties, and photodynamic inactivation of *Escherichia coli* using a cationic and a noncharged Zn(II) pyridyloxyphthalocyanine derivatives. Bioorg Med Chem 2005;13:3037–45.
[26] Segalla A, Borsarelli CD, Braslavski SE, Spikes JD, Roncucci G, Dei D, et al. Photophysical, photochemical and antibacterial photosensitizing properties of a novel octacationic Zn(II)-phthalocyanine. Photochem Photobiol Sci 2002;1:641–8.
[27] Wood SR, Holroyd JA, Brown SB. The subcellular localization of Zn(II) phthalocyanines and their redistribution on exposure to light. Photochem Photobiol 1997;65:397–402.
[28] Castano AP, Demidova TN, Hamblin MR. Mechanisms in photodynamic therapy: part one – photosensitizers, photochemistry and cellular localization. Photodiagn Photodyn Ther 2004;1:279–93.
[29] Kessel D. Correlation between subcellular localization and photodynamic efficacy. J Porphyrins Phthalocyanines 2004;8:1009–14.
[30] Weber JH, Busch DH. Complexes derived from strong field ligands XIX: magnetic properties of transition metal derivatives of 4,4′,4″,4‴-tetrasulfophthalocyanine. Inorg Chem 1965;4:469–71.
[31] Perrin DD, Armarego WLF. Purification of laboratory chemicals. 2nd ed. Oxford: Pergamon Press; 1989.
[32] Wöhrle D, Eskes M, Shigehara K, Yamada A. A simple synthesis of 4,5-disubstituted 1,2-dicyanobenzenes and 2,3,9,10,16,17,23,24-octasubstituted phthalocyanines. Synthesis 1993:194–6.
[33] Li H, Jensen TJ, Fronczek FR, Vicente MGH. Syntheses and properties of a series of cationic water-soluble phthalocyanines. J Med Chem 2008;51:502–11.
[34] Du HR, Fuh A, Li J, Corkan LA, Lindsey JS. PhotochemCAD: a computer-aided design and research tool in photochemistry. Photochem Photobiol 1998;68:141–2.
[35] Strickler SJ, Berg RA. Relationship between absorption intensity and fluorescence lifetime of molecules. J Chem Phys 1962;37:814–22.
[36] Smith TD, Livorness J, Taylor H, Pilbrow JR, Sinclair GR. Physico-chemical study of copper(II) and cobalt(II) chelates of tetra-2,3-pyridinoporphyrazine. J Chem Soc Dalton Trans 1983;:1391–400.
[37] Ogunsipe A, Nyokong T. Effects of central metal on the photophysical and photochemical properties of non-transition metal sulfophthalocyanine. J Porphyrins Phthalocyanines 2005;9:121–9.
[38] Fery-Forgues S, Lavabre D. Are fluorescence quantum yields so tricky to measure? A demonstration using familiar stationery products. J Chem Educ 1999;76:1260–4.
[39] Montalban A, Meunier H, Ostler R, Barrett A, Hoffman B, Rumbles G. Photoperoxidation of a diamino zinc porphyrazine to the seco-zinc porphyrazine: suicide or murder. J Phys Chem A 1999;103:4352–8.
[40] Kubát P, Mosinger J. Photophysical properties of metal complexes of meso-tetrakis(4-sulphonatophenyl) porphyrin. J Photochem Photobiol A Chem 1996;96:93–7.
[41] Tran-Thi TH, Desforge C, Thiec C. Singlet–singlet and triplet–triplet intramolecular transfer processes in a covalently linked porphyrin–phthalocyanine heterodimer. J Phys Chem 1989;93:1226–33.
[42] Harriman A, Richoux MC. Attempted photoreduction of hydrogen using sulphophthalocyanines as chromophores for three-component systems. J Chem Soc Faraday Trans 2 1980;76:1618–26.

[43] Bonnet R, Ridge RJ, Land EJ, Sinclair RS, Tait D, Truscott TG. Pulsed irradiation of water-soluble porphyrins. J Chem Soc Faraday Trans 1 1982;78: 127–36.
[44] Tau P, Ogunsipe AO, Maree S, Maree MD, Nyokong T. Influence of cyclodextrins on the fluorescence, photostability and singlet oxygen quantum yields of zinc phthalocyanine and naphthalocyanine complexes. J Porphyrins Phthalocyanines 2003;7:439–46.
[45] Seotsanyana-Mokhosi I, Kuznetsova N, Nyokong T. Photochemical studies of tetra-2,3-pyridinoporphyrazines. J Photochem Photobiol A Chem 2001;140:215–22.
[46] Ogunsipe A, Maree D, Nyokong T. Solvent effects on the photochemical and fluorescence properties of zinc phthalocyanine derivatives. J Mol Struct 2003;650:131–40.
[47] Wilkinson F, Helman WP, Ross AB. Quantum yields for the photosensitized formation of the lowest electronically excited singlet state of molecular oxygen in solution. J Phys Chem Ref Data 1993;22:113–262.
[48] Kuznetsova N, Gretsova N, Kalmykova E, Makarova E, Dashkevich S, Negrimovskii V, et al. Russ J Gen Chem 2000;70:133–40.
[49] Spliller W, Kliesch H, Wöhrle W, Hackbarth S, Röder B, Schnurpfeil G. Singlet oxygen quantum yields of different photosensitizers in polar solvents and micellar solutions. J Porphyrins Phthalocyanines 1999;2:145–58.
[50] Kuznetsova N, Okunchikov VV, Derkacheva VM, Kaliya O, Lukyanets E. Photooxidation of metallophthalocyanines: the effects of singlet oxygen and PcM-O_2 complex formation. J Porphyrins Phthalocyanines 2005;9:393–7.
[51] Gaspard S, Maillard P. Structure des phtalocyanines tetra tertio-butylees: mecanisme de la synthese. Tetrahedron 1987;43:1083–90.
[52] Maclean AL, Foran GJ, Kennedy BJ, Turner P, Hambley TW. Structural characterization of nickel(II) tetraphenylporphyrin. Aust J Chem 1996;49:1273–8.
[53] Kobayashi N, Fukuda T, Ueno K, Ogino H. Extremely non-planar phthalocyanines with saddle or helical conformation: synthesis and structural characterizations. J Am Chem Soc 2001;123:10740–1.
[54] Schmidt R. Influence of heavy atoms on the deactivation of singlet oxygen ($^1\Delta g$) in solution. J Am Chem Soc 1989;111:6983–7.
[55] Nilsson R, Kearns DR. Role of singlet oxygen in some chemiluminescence and enzyme oxidation reactions. J Phys Chem 1974;78:1681–3.